The $\Upsilon(1S) \to B_c \rho$ decay with perturbative QCD approach

Junfeng Sun,[1] Yueling Yang,[1] Qingxia Li,[1] Gongru Lu,[1] Jinshu Huang,[2] and Qin Chang[1]

[1] *Institute of Particle and Nuclear Physics,*
College of Physics and Electronic Engineering,
Henan Normal University, Xinxiang 453007, China

[2] *College of Physics and Electronic Engineering,*
Nanyang Normal University, Nanyang 473061, China

Abstract

With the potential prospects of the $\Upsilon(1S)$ data samples at the running LHC and upcoming SuperKEKB, the $\Upsilon(1S) \to B_c \rho$ weak decays are studied with the pQCD approach. It is found that (1) the lion's share of branching ratio comes from the longitudinal polarization helicity amplitudes; (2) branching ratio for the $\Upsilon(1S) \to B_c \rho$ decay can reach up to $\mathcal{O}(10^{-9})$, which might be hopefully measurable.

I. INTRODUCTION

The $\Upsilon(1S)$ meson consists of the bottom quark and antiquark pair $b\bar{b}$, carries the definitely established quantum numbers of $I^G J^{PC} = 0^- 1^{--}$ [1], and lies below the kinematic $B\bar{B}$ threshold. The $\Upsilon(1S)$ meson decay mainly through the strong interaction, the electromagnetic interaction and radiative transition. Besides, the $\Upsilon(1S)$ meson can also decay via the weak interactions within the standard model. More than 10^8 $\Upsilon(1S)$ data samples have been accumulated at Belle [2]. More and more upsilon data samples with high precision are promisingly expected at the running LHC and the forthcoming SuperKEKB. Although the branching ratio for the $\Upsilon(1S)$ weak decay is tiny, it seems to exist a realistic possibility to search for the signals of the $\Upsilon(1S)$ weak decay at future experiments. In this paper, we will study the $\Upsilon(1S) \to B_c\rho$ weak decay with the perturbative QCD (pQCD) approach [3–5].

Experimentally, there is no report on the $\Upsilon(1S) \to B_c\rho$ weak decay so far. The signals for the $\Upsilon(1S) \to B_c\rho$ weak decay should, in principle, be easily identified, due to the facts that the final states have opposite electric charges, have definite momentum and energy, and are back-to-back in the rest frame of the $\Upsilon(1S)$ meson. In addition, the identification of a single flavored B_c meson could be used to effectively enhance signal-to-background ratio. Another important and fashionable motivation is that evidences of an abnormally large branching ratio for the $\Upsilon(1S)$ weak decay might be a hint of new physics.

Theoretically, the $\Upsilon(1S) \to B_c\rho$ weak decay belongs to the external W emission topography, and is favored by the Cabibbo-Kabayashi-Maskawa (CKM) matrix elements $|V_{cb}V_{ud}^*|$. So it should have relatively large branching ratio among the $\Upsilon(1S)$ weak decays, which has been studied with the naive factorization (NF) approximation [6, 7]. Recently, some attractive methods have been developed, such as the pQCD approach [3–5], the QCD factorization approach [8–10], soft and collinear effective theory [11–14], and applied widely to accommodate measurements on the B meson weak decays. The $\Upsilon(1S) \to B_c\rho$ decay permit one to cross check parameters obtained from the B meson decay, to test the practical applicability of various phenomenological models in the vector meson weak decays, and to further explore the underlying dynamical mechanism of the heavy quark weak decay.

This paper is organized as follows. In section II, we present the theoretical framework and the amplitudes for the $\Upsilon(1S) \to B_c\rho$ decay with the pQCD approach. Section III is devoted to numerical results and discussion. The last section is our summary.

II. THEORETICAL FRAMEWORK

A. The effective Hamiltonian

The effective Hamiltonian responsible for the $\Upsilon(1S) \to B_c\rho$ weak decay is [15]

$$\mathcal{H}_{\rm eff} \ = \ \frac{G_F}{\sqrt{2}} V_{cb} V_{ud}^{*} \Big\{ C_1(\mu)\, Q_1(\mu) + C_2(\mu)\, Q_2(\mu) \Big\} + \text{H.c.}, \tag{1}$$

where $G_F \simeq 1.166{\times}10^{-5}\,\text{GeV}^{-2}$ [1] is the Fermi coupling constant; the CKM factor is written as a power series in the Wolfenstein parameter $\lambda \simeq 0.2$ [1],

$$V_{cb} V_{ud}^{*} \ = \ A\lambda^2 - \frac{1}{2}A\lambda^4 - \frac{1}{8}A\lambda^6 + \mathcal{O}(\lambda^8). \tag{2}$$

The local operators are defined as follows.

$$Q_1 \ = \ [\bar{c}_{\alpha}\gamma_{\mu}(1-\gamma_5)b_{\alpha}][\bar{q}_{\beta}\gamma^{\mu}(1-\gamma_5)u_{\beta}], \tag{3}$$

$$Q_2 \ = \ [\bar{c}_{\alpha}\gamma_{\mu}(1-\gamma_5)b_{\beta}][\bar{q}_{\beta}\gamma^{\mu}(1-\gamma_5)u_{\alpha}], \tag{4}$$

where α and β are color indices.

From Eq.(1), it is clearly seen that only the tree operators contribute to the concerned process, and there is no pollution from penguin and annihilation contributions. As it is well known, the Wilson coefficients $C_{1,2}(\mu)$ summarize the physical contributions above the scales of μ, and could be properly calculated with the renormalization group assisted perturbation theory. The physical contributions below the scales of μ are included in the hadronic matrix elements (HME) where the local operators sandwiched between initial and final hadron states. The most complicated part is the treatment on HME, where the perturbative and nonperturbative effects entangle with each other. To obtain the decay amplitudes, the remaining work is to calculate HME properly.

B. Hadronic matrix elements

With the Lepage-Brodsky approach for exclusive processes [16], HME could be expressed as the convolution of hard scattering subamplitudes containing perturbative contributions with the universal wave functions reflecting the nonperturbative contributions. To eliminate the endpoint singularities appearing in the collinear factorization approximation, the pQCD approach suggests [3–5] retaining the transverse momentum of quarks and introducing the

Sudakov factor. Finally, the decay amplitudes could be factorized into three parts [4, 5]: the hard effects enclosed by the Wilson coefficients C_i, the heavy quark decay subamplitudes $\mathcal{H}$, and the universal wave functions Φ,

$$\int dk\, C_i(t)\, \mathcal{H}(t,k)\, \Phi(k)\, e^{-S}, \tag{5}$$

where t is a typical scale, k is the momentum of the valence quarks, and the Sudakov factor e^{-S} can effectively suppress the long-distance contributions and make the hard scattering more perturbative.

C. Kinematic variables

The light cone kinematic variables in the $\Upsilon(1S)$ rest frame are defined as follows.

$$p_{\Upsilon} = p_1 = \frac{m_1}{\sqrt{2}}(1,1,0), \tag{6}$$

$$p_{B_c} = p_2 = (p_2^+, p_2^-, 0), \tag{7}$$

$$p_{\rho} = p_3 = (p_3^-, p_3^+, 0), \tag{8}$$

$$k_i = x_i\, p_i + (0, 0, \vec{k}_{i\perp}), \tag{9}$$

$$\epsilon_i^{\parallel} = \frac{p_i}{m_i} - \frac{m_i}{p_i{\cdot}n_+} n_+, \tag{10}$$

$$\epsilon_i^{\perp} = (0, 0, \vec{1}), \tag{11}$$

$$n_+ = (1, 0, 0), \tag{12}$$

$$p_i^{\pm} = (E_i \pm p)/\sqrt{2}, \tag{13}$$

$$s = 2\, p_2{\cdot}p_3, \tag{14}$$

$$t = 2\, p_1{\cdot}p_2 = 2\, m_1\, E_2, \tag{15}$$

$$u = 2\, p_1{\cdot}p_3 = 2\, m_1\, E_3, \tag{16}$$

$$p = \frac{\sqrt{[m_1^2 - (m_2+m_3)^2]\,[m_1^2 - (m_2-m_3)^2]}}{2\, m_1}, \tag{17}$$

where x_i and $\vec{k}_{i\perp}$ are the longitudinal momentum fraction and transverse momentum of the valence quark, respectively; $\epsilon_i^{\parallel}$ and $\epsilon_i^{\perp}$ are the longitudinal and transverse polarization vectors, respectively, satisfying with the relations $\epsilon_i^2 = -1$ and $\epsilon_i{\cdot}p_i = 0$; the subscript i = 1, 2, 3 on variables p_i, E_i, m_i, and $\epsilon_i^{\parallel,\perp}$ correspond to the $\Upsilon(1S)$, B_c and ρ mesons, respectively; n_+ is the null vector; s, t and u are the Lorentz-invariant variables; p is the common momentum of final states. The notation of momentum is displayed in Fig.1(a).

D. Wave functions

With the notation in [17, 18], the definitions of the diquark operator HME are

$$\langle 0|b_i(z)\bar{b}_j(0)|\Upsilon(p_1,\epsilon_1^{\parallel})\rangle \;=\; \frac{f_{\Upsilon}}{4}\int d^4k_1\, e^{-ik_1\cdot z}\Big\{\not{\epsilon}_1^{\parallel}\Big[m_1\,\Phi_{\Upsilon}^{v}(k_1)-\not{p}_1\,\Phi_{\Upsilon}^{t}(k_1)\Big]\Big\}_{ji}, \tag{18}$$

$$\langle 0|b_i(z)\bar{b}_j(0)|\Upsilon(p_1,\epsilon_1^{\perp})\rangle \;=\; \frac{f_{\Upsilon}}{4}\int d^4k_1\, e^{-ik_1\cdot z}\Big\{\not{\epsilon}_1^{\perp}\Big[m_1\,\Phi_{\Upsilon}^{V}(k_1)-\not{p}_1\,\Phi_{\Upsilon}^{T}(k_1)\Big]\Big\}_{ji}, \tag{19}$$

$$\langle B_c^{+}(p_2)|\bar{c}_i(z)b_j(0)|0\rangle \;=\; \frac{i}{4}f_{B_c}\int dx_2\, e^{ix_2p_2\cdot z}\,\Big\{\gamma_5\Big[\not{p}_2+m_2\Big]\phi_{B_c}(x_2)\Big\}_{ji}, \tag{20}$$

$$\langle \rho^{-}(p_3,\epsilon_3^{\parallel})|u_i(0)\bar{d}_j(z)|0\rangle \;=\; \frac{1}{4}\int_0^1 dk_3\, e^{ik_3\cdot z}\Big\{\not{\epsilon}_3^{\parallel}\,m_3\,\Phi_{\rho}^{v}(k_3)+\not{\epsilon}_3^{\parallel}\not{p}_3\,\Phi_{\rho}^{t}(k_3)+m_3\,\Phi_{\rho}^{s}(k_3)\Big\}_{ji}, \tag{21}$$

$$\begin{aligned}\langle \rho(p_3,\epsilon_3^{\perp})|u_i(0)\bar{d}_j(z)|0\rangle \;=\;& \frac{1}{4}\int_0^1 dk_3\, e^{ik_3\cdot z}\Big\{\,\not{\epsilon}_3^{\perp}m_3\,\Phi_{\rho}^{V}(k_3)\\ &+\not{\epsilon}_3^{\perp}\,\not{p}_3\,\Phi_{\rho}^{T}(k_3)+\frac{i\,m_3}{p_3{\cdot}n_+}\varepsilon_{\mu\nu\alpha\beta}\,\gamma_5\,\gamma^{\mu}\,\epsilon_3^{\perp,\nu}\,p_3^{\alpha}\,n_+^{\beta}\,\Phi_{\rho}^{A}(k_3)\Big\}_{ji},\end{aligned} \tag{22}$$

where f_{Υ} and f_{B_c} are decay constants; the definitions of wave functions $\Phi_{\rho}^{v,t,s}$ and $\Phi_{\rho}^{V,T,A}$ can be found in Ref. [17, 18]. In fact, for the ρ meson, only three wave functions Φ_{ρ}^{v} and $\Phi_{\rho}^{V,A}$ are involved in the decay amplitudes (see Appendix A). The twist-2 distribution amplitude for the longitudinal polarization ρ meson is [17, 18]:

$$\phi_{\rho}^{v}(x) \;=\; f_{\rho}\,6\,x\,\bar{x}\sum_{i=0} a_{2i}^{\parallel}\,C_{2i}^{3/2}(t), \tag{23}$$

where f_{ρ} is the decay constant; $\bar{x}=1-x$; $t=\bar{x}-x$; $a_i^{\parallel}$ and $C_i^{3/2}(t)$ are the Gegenbauer moment and polynomial, respectively; $a_i^{\parallel}=0$ for odd i due to the G-parity invariance of the ρ distribution amplitudes. For the twist-3 distribution amplitudes of the transverse polarization ρ meson, for simplicity, we will take the asymptotic forms [17, 18]:

$$\phi_{\rho}^{V}(x) \;=\; f_{\rho}\,\frac{3}{4}\,(1+t^2), \tag{24}$$

$$\phi_{\rho}^{A}(x) \;=\; f_{\rho}\,\frac{3}{2}\,(-t). \tag{25}$$

Because of $m_{\Upsilon(1S)}\simeq 2m_b$ and $m_{B_c}\simeq m_b+m_c$, both $\Upsilon(1S)$ and B_c systems are nearly nonrelativistic. Nonrelativistic quantum chromodynamics (NRQCD) [19–21] and Schrödinger equation can be used to describe their spectrum. The eigenfunction of the time-independent Schrödinger equation with scalar harmonic oscillator potential corresponding to the quantum numbers $nL=1S$ is written as

$$\phi(\vec{k}) \sim e^{-\vec{k}^2/2\beta^2}, \tag{26}$$

where parameter β determines the average transverse momentum, i.e., $\langle 1S|\vec{k}_\perp^2|1S\rangle = \beta^2$. Employing the substitution ansatz [22],

$$\vec{k}^2 \to \frac{1}{4}\sum_i \frac{\vec{k}_{i\perp}^2 + m_{q_i}^2}{x_i}, \tag{27}$$

where x_i, $\vec{k}_{i\perp}$, m_{q_i} are the longitudinal momentum fraction, transverse momentum, mass of the valence quarks in hadrons, respectively, with the relations $\sum x_i = 1$ and $\sum \vec{k}_{i\perp} = 0$, then integrating out $\vec{k}_{i\perp}$ and combining with their asymptotic forms, one can obtain [17, 23]

$$\phi_{B_c}(x) = A\, x\bar{x} \exp\Big\{ - \frac{\bar{x}\, m_c^2 + x\, m_b^2}{8\, \beta_2^2\, x\, \bar{x}} \Big\}, \tag{28}$$

$$\phi_\Upsilon^v(x) = \phi_\Upsilon^T(x) = B\, x\bar{x} \exp\Big\{ - \frac{m_b^2}{8\, \beta_1^2\, x\, \bar{x}} \Big\}, \tag{29}$$

$$\phi_\Upsilon^t(x) = C\, t^2 \exp\Big\{ - \frac{m_b^2}{8\, \beta_1^2\, x\, \bar{x}} \Big\}, \tag{30}$$

$$\phi_\Upsilon^V(x) = D\, (1 + t^2) \exp\Big\{ - \frac{m_b^2}{8\, \beta_1^2\, x\, \bar{x}} \Big\}, \tag{31}$$

where $\beta_i = \xi_i \alpha_s(\xi_i)$ with $\xi_i = m_i/2$ based on the NRQCD power counting rules [19]; parameters A, B, C, D are the normalization coefficients satisfying the conditions

$$\int_0^1 dx\, \phi_{B_c}(x) = 1, \quad \int_0^1 dx\, \phi_\Upsilon^{v,t}(x) = \int_0^1 dx\, \phi_\Upsilon^{V,T}(x) = 1. \tag{32}$$

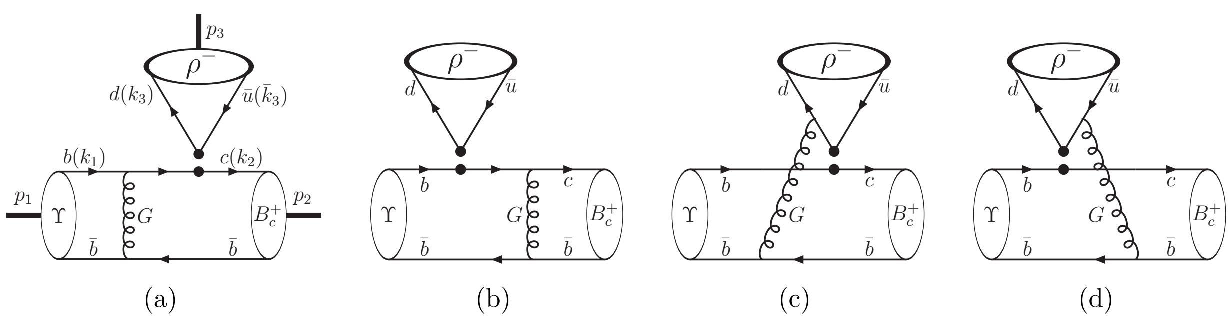

FIG. 1: Feynman diagrams for the $\Upsilon \to B_c\rho$ decay with the pQCD approach, where (a) and (b) are factorizable emission diagrams, (c) and (d) are nonfactorizatble emission diagrams.

E. Decay amplitudes

The Feynman diagrams for the $\Upsilon(1S) \to B_c\rho$ decay are shown in Fig.1, including factorizable emission topologies (a) and (b) where gluon connects to the quarks in the same meson, and nonfactorizable emission topologies (c) and (d) where gluon attaches to the quarks in two different mesons.

The amplitude for the $\Upsilon(1S) \to B_c\rho$ decay is defined as below [24],

$$\mathcal{A}(\Upsilon(1S){\to}B_c\rho) \;=\; \mathcal{A}_L(\epsilon_1^{\parallel},\epsilon_3^{\parallel}) + \mathcal{A}_N(\epsilon_1^{\perp},\epsilon_3^{\perp}) + i\,\mathcal{A}_T\,\varepsilon_{\mu\nu\alpha\beta}\,\epsilon_1^{\mu}\,\epsilon_3^{\nu}\,p_1^{\alpha}\,p_3^{\beta}, \tag{33}$$

which is conventionally written as the helicity amplitudes [24],

$$\mathcal{A}_0 \;=\; -C_{\mathcal{A}}\sum_i \mathcal{A}_L^i(\epsilon_1^{\parallel},\epsilon_3^{\parallel}), \tag{34}$$

$$\mathcal{A}_{\parallel} \;=\; \sqrt{2}\,C_{\mathcal{A}}\sum_i \mathcal{A}_N^i(\epsilon_1^{\perp},\epsilon_3^{\perp}), \tag{35}$$

$$\mathcal{A}_{\perp} \;=\; \sqrt{2}\,C_{\mathcal{A}}\,m_1\,p\sum_i \mathcal{A}_T^i, \tag{36}$$

$$C_{\mathcal{A}} \;=\; i\frac{G_F}{\sqrt{2}}\,\frac{C_F}{N}\,\pi\,f_{\Upsilon}\,f_{B_c}\,V_{cb}V_{ud}^{*}, \tag{37}$$

where $C_F = 4/3$ and the color number $N = 3$; the the superscript i on $\mathcal{A}_{L,N,T}^i$ corresponds to the indices of Fig.1. The explicit expressions of building blocks $\mathcal{A}_{L,N,T}^i$ are collected in Appendix A.

III. NUMERICAL RESULTS AND DISCUSSION

In the rest frame of the $\Upsilon(1S)$ meson, branching ratio ($\mathcal{B}r$), polarization fractions ($f_{0,\parallel,\perp}$) and relative phase between helicity amplitudes ($\phi_{\parallel,\perp}$) for the $\Upsilon(1S) \to B_c\rho$ weak decay are defined as

$$\mathcal{B}r \;=\; \frac{1}{12\pi}\,\frac{p}{m_{\Upsilon}^2\Gamma_{\Upsilon}}\,\Big\{|\mathcal{A}_0|^2 + |\mathcal{A}_{\parallel}|^2 + |\mathcal{A}_{\perp}|^2\Big\}, \tag{38}$$

$$f_{0,\parallel,\perp} \;=\; \frac{|\mathcal{A}_{0,\parallel,\perp}|^2}{|\mathcal{A}_0|^2 + |\mathcal{A}_{\parallel}|^2 + |\mathcal{A}_{\perp}|^2}, \tag{39}$$

$$\phi_{\parallel,\perp} \;=\; \arg(\mathcal{A}_{\parallel,\perp}/\mathcal{A}_0), \tag{40}$$

where mass $m_{\Upsilon(1S)} = 9460.30{\pm}0.26$ MeV and decay width $\Gamma_{\Upsilon} = 54.02{\pm}1.25$ keV [1].

The values of other input parameters are listed as follows. If not specified explicitly, we will take their central values as default inputs.

(1) Wolfenstein parameters [1]: $A = 0.814^{+0.023}_{-0.024}$ and $\lambda = 0.22537{\pm}0.00061$.

(2) Masses of quarks [1]: $m_c = 1.67{\pm}0.07$ GeV and $m_b = 4.78{\pm}0.06$ GeV.

(3) Gegenbauer moments $a_0^{\parallel} = 1$ and $a_2^{\parallel} = 0.15{\pm}0.07$ for twist-2 distribution amplitudes of the ρ meson [18].

(4) Decay constants: $f_{\Upsilon} = (676.4{\pm}10.7)$ MeV [23], $f_{B_c} = 489{\pm}5$ MeV [25], $f_{\rho} = 216{\pm}3$ MeV [18].

Our numerical results are presented as follows.

$$\mathcal{B}r \;=\; (8.34^{+0.47+1.35+0.40+1.44}_{-0.69-0.88-0.40-1.26})\times 10^{-9}, \tag{41}$$

$$f_0 \;=\; (82.2^{+0.0+1.1+0.0}_{-0.7-1.3-0.0})\%, \tag{42}$$

$$f_{\parallel} \;=\; (15.0^{+0.6+1.0+0.0}_{-0.0-0.8-0.0})\%, \tag{43}$$

$$f_{\perp} \;=\; (2.8^{+0.1+0.3+0.0}_{-0.0-0.3-0.0})\%, \tag{44}$$

$$\phi_{\parallel} \simeq 0, \qquad \phi_{\perp} \simeq \pi, \tag{45}$$

where the first uncertainty comes from the choice of the typical scale $(1{\pm}0.1)t_i$, and the expression t_i is given in Eq.(A24) and Eq.(A25); the second uncertainty is from masses m_b and m_c; the third uncertainty is from hadronic parameters including decay constants and Gegenbauer moments; and the fourth uncertainty of branching ratio comes from the CKM parameters. The following are some comments.

(1) The branching ratio is about two or three orders of magnitude larger than the previous estimation [6, 7] with the NF approximation. Many factors lead to this large difference. For example, the values of Wilson coefficients are dynamically enhanced due to the choice of typical scale within the pQCD framework [24]. Both factorizable and nonfactorizable effects contribute to the decay amplitudes with the pQCD approach, while only factorizable contributions are considered with the NF approximation, and so on. Anyway, these different predictions should be examined by the future experiments.

(2) Branching ratio for the $\Upsilon(1S) \to B_c\rho$ decay can reach up to $\mathcal{O}(10^{-9})$ with the pQCD approach, which might be measurable at the running LHC and forthcoming SuperKEKB. For example, the $\Upsilon(1S)$ production cross section in p-Pb collision is about a few μb at LHCb [26] and ALICE [27]. Over 10^{12} $\Upsilon(1S)$ data samples per ab^{-1} data collected at LHCb and ALICE are in principle available, corresponding to a few thousands of the $\Upsilon(1S) \to B_c\rho$ events.

(3) There is a hierarchical pattern among the longitudinal f_0, parallel $f_{\parallel}$, and perpendicular $f_{\perp}$ polarization fractions, i.e.,

$$f_0 : f_{\parallel} : f_{\perp} \simeq 1 : \frac{p}{\sqrt{2} m_{\Upsilon(1S)}} : \frac{p^2}{2 m_{\Upsilon(1S)}^2}, \tag{46}$$

where p is the common momentum of final state in the rest frame of the $\Upsilon(1S)$ meson. The relation Eq.(46) is basically agree with previous estimation [7]. It means that the contributions to branching ratio for the $\Upsilon(1S) \to B_c \rho$ decay mainly come from the longitudinal polarization fractions, because of $f_0 > f_{\parallel} > f_{\perp}$.

(4) The relative phase $\phi_{\parallel}$ is close to zero. The reason is that the factorizable contributions from diagrams Fig.1(a,b) is real and proportional to the large coefficient a_1, while the nonfactorizable contributions from diagrams Fig.1(c,d) is suppressed by the color factor and proportional to the small Wilson coefficient C_2, and the strong phases arise only from the nonfactorizable contributions, which is consistent with the prediction of the QCD factorization approach [8, 9] where the strong phase arising from nonfactorizable contributions is suppressed by color and α_s for the a_1-dominated processes. The relative phases, if they could be determined experimentally, will improve our understanding on the strong interactions.

IV. SUMMARY

The $\Upsilon(1S)$ weak decay is allowable within the standard model. In this paper, the $\Upsilon(1S) \to B_c \rho$ weak decays are studied with the pQCD approach. It is found that with the nonrelativistic wave functions for $\Upsilon(1S)$ and B_c mesons, the longitudinal polarization fraction is the largest one, and branching ratios for the $\Upsilon(1S) \to B_c \rho$ decay can reach up to $\mathcal{O}(10^{-9})$, which might be detectable at the future experiments.

Acknowledgments

We thank Professor Dongsheng Du (IHEP@CAS) and Professor Yadong Yang (CCNU) for helpful discussion. The work is supported by the National Natural Science Foundation of China (Grant Nos. 11547014, U1232101, U1332103 and 11275057).

Appendix A: Building blocks of decay amplitudes

For the sake of simplicity, the amplitude for the $\Upsilon(1S) \to B_c \rho$ decay, Eq.(33), is decomposed into building blocks $\mathcal{A}^i_{L,N,T}$, where the superscript i corresponds to the indices of Fig.1. With the pQCD master formula Eq.(5), the explicit expressions of $\mathcal{A}^i_{L,N,T}$ are written as follows.

$$\begin{aligned}
\mathcal{A}^a_L &= \int_0^1 dx_1 \int_0^1 dx_2 \int_0^\infty b_1 db_1 \int_0^\infty b_2 db_2\, \phi^v_\Upsilon(x_1) \\
&\quad \phi_{B_c}(x_2)\, E_f(t_a)\, \alpha_s(t_a)\, a_1(t_a)\, H_f(\alpha_e, \beta_a, b_1, b_2) \\
&\quad \Big\{ m_1^2\, s + m_2\, m_b\, u - (4\, m_1^2\, p^2 + m_2^2\, u)\, \bar{x}_2 \Big\}, \qquad \text{(A1)} \\
\mathcal{A}^a_N &= m_1\, m_3 \int_0^1 dx_1 \int_0^1 dx_2 \int_0^\infty b_1 db_1 \int_0^\infty b_2 db_2\, \phi^V_\Upsilon(x_1) \\
&\quad \phi_{B_c}(x_2)\, E_f(t_a)\, \alpha_s(t_a)\, a_1(t_a)\, H_f(\alpha_e, \beta_a, b_1, b_2) \\
&\quad \Big\{ 2\, m_2^2\, \bar{x}_2 - 2\, m_2\, m_b - t \Big\}, \qquad \text{(A2)} \\
\mathcal{A}^a_T &= 2\, m_1\, m_3 \int_0^1 dx_1 \int_0^1 dx_2 \int_0^\infty b_1 db_1 \int_0^\infty b_2 db_2\, \phi^V_\Upsilon(x_1) \\
&\quad \phi_{B_c}(x_2)\, E_f(t_a)\, \alpha_s(t_a)\, a_1(t_a)\, H_f(\alpha_e, \beta_a, b_1, b_2), \qquad \text{(A3)}
\end{aligned}$$

$$\begin{aligned}
\mathcal{A}^b_L &= \int_0^1 dx_1 \int_0^1 dx_2 \int_0^\infty b_1 db_1 \int_0^\infty b_2 db_2 \\
&\quad \phi_{B_c}(x_2)\, E_f(t_b)\, \alpha_s(t_b)\, a_1(t_b) H_f(\alpha_e, \beta_b, b_2, b_1) \\
&\quad \Big\{ \phi^v_\Upsilon(x_1) \Big[m_1^2\, (s - 4\, p^2)\, \bar{x}_1 + 2\, m_2\, m_c\, u - m_2^2\, u \Big] \\
&\quad + \phi^t_\Upsilon(x_1)\, m_1 \Big[s\, (2\, m_2 - m_c) - 2\, m_2\, u\, \bar{x}_1 \Big] \Big\}, \qquad \text{(A4)} \\
\mathcal{A}^b_N &= m_3 \int_0^1 dx_1 \int_0^1 dx_2 \int_0^\infty b_1 db_1 \int_0^\infty b_2 db_2 \\
&\quad \phi_{B_c}(x_2)\, E_f(t_b)\, \alpha_s(t_b)\, a_1(t_b)\, H_f(\alpha_e, \beta_b, b_2, b_1) \\
&\quad \Big\{ \phi^V_\Upsilon(x_1)\, m_1 \Big[2\, m_2^2 - 4\, m_2\, m_c - t\, \bar{x}_1 \Big] \\
&\quad + \phi^T_\Upsilon(x_1) \Big[t\, (m_c - 2\, m_2) + 4\, m_1^2\, m_2\, \bar{x}_1 \Big] \Big\}, \qquad \text{(A5)} \\
\mathcal{A}^b_T &= -2\, m_3 \int_0^1 dx_1 \int_0^1 dx_2 \int_0^\infty b_1 db_1 \int_0^\infty b_2 db_2 \\
&\quad \phi_{B_c}(x_2)\, E_f(t_b)\, \alpha_s(t_b)\, a_1(t_b)\, H_f(\alpha_e, \beta_b, b_2, b_1) \\
&\quad \Big\{ \phi^V_\Upsilon(x_1)\, m_1\, \bar{x}_1 + \phi^T_\Upsilon(x_1)\, (m_c - 2\, m_2) \Big\}, \qquad \text{(A6)}
\end{aligned}$$

$$\begin{aligned}
\mathcal{A}^c_L &= \frac{1}{N_c} \int_0^1 dx_1 \int_0^1 dx_2 \int_0^1 dx_3 \int_0^\infty db_1 \int_0^\infty b_2 db_2 \int_0^\infty b_3 db_3 \\
&\quad \phi_{B_c}(x_2)\, \phi^v_\rho(x_3)\, E_n(t_c)\, \alpha_s(t_c)\, C_2(t_c)\, H_n(\alpha_e, \beta_c, b_2, b_3)
\end{aligned}$$

$$\delta(b_1-b_2)\Big\{\phi_\Upsilon^v(x_1)\,u\Big[t\,x_1-2\,m_2^2\,x_2-s\,\bar{x}_3\Big]$$
$$+\phi_\Upsilon^t(x_1)\,m_1\,m_2\Big[s\,x_2+2\,m_3^2\,\bar{x}_3-u\,x_1\Big]\Big\}, \tag{A7}$$

$$\begin{aligned}\mathcal{A}_N^c = {} & \frac{m_3}{N_c}\int_0^1 dx_1\int_0^1 dx_2\int_0^1 dx_3\int_0^\infty db_1\int_0^\infty b_2 db_2\int_0^\infty b_3 db_3 \\ & \phi_{B_c}(x_2)\,E_n(t_c)\,\alpha_s(t_c)\,C_2(t_c)\,H_n(\alpha_e,\beta_c,b_2,b_3) \\ & \Big\{\phi_\Upsilon^V(x_1)\,\phi_\rho^V(x_3)\,m_1\Big[2\,s\,\bar{x}_3+4\,m_2^2\,x_2-2\,t\,x_1\Big] \\ & +\phi_\Upsilon^T(x_1)\,\phi_\rho^V(x_3)\,m_2\Big[2\,m_1^2\,x_1-t\,x_2-u\,\bar{x}_3\Big] \\ & +\phi_\Upsilon^T(x_1)\,\phi_\rho^A(x_3)\,2\,m_1\,m_2\,p\,(x_2-\bar{x}_3)\Big\}\,\delta(b_1-b_2),\end{aligned} \tag{A8}$$

$$\begin{aligned}\mathcal{A}_T^c = {} & \frac{m_3}{N_c\,p}\int_0^1 dx_1\int_0^1 dx_2\int_0^1 dx_3\int_0^\infty db_1\int_0^\infty b_2 db_2\int_0^\infty b_3 db_3 \\ & \phi_{B_c}(x_2)\,E_n(t_c)\,\alpha_s(t_c)\,C_2(t_c)\,H_n(\alpha_e,\beta_c,b_2,b_3) \\ & \Big\{\phi_\Upsilon^V(x_1)\,\phi_\rho^A(x_3)\Big[2\,s\,\bar{x}_3+4\,m_2^2\,x_2-2\,t\,x_1\Big] \\ & +\phi_\Upsilon^T(x_1)\,\phi_\rho^A(x_3)\,r_2\Big[2\,m_1^2\,x_1-t\,x_2-u\,\bar{x}_3\Big] \\ & +2\,m_2\,p\,\phi_\Upsilon^T(x_1)\,\phi_\rho^V(x_3)\,(x_2-\bar{x}_3)\Big\}\,\delta(b_1-b_2),\end{aligned} \tag{A9}$$

$$\begin{aligned}\mathcal{A}_L^d = {} & \frac{1}{N_c}\int_0^1 dx_1\int_0^1 dx_2\int_0^1 dx_3\int_0^\infty db_1\int_0^\infty b_2 db_2\int_0^\infty b_3 db_3 \\ & \phi_{B_c}(x_2)\,\phi_\rho^v(x_3)\,E_n(t_d)\,\alpha_s(t_d)\,C_2(t_d)\,H_n(\alpha_e,\beta_d,b_2,b_3) \\ & \delta(b_1-b_2)\Big\{\phi_\Upsilon^t(x_1)\,m_1\,m_2\Big[s\,x_2+2\,m_3^2\,x_3-u\,x_1\Big] \\ & +\phi_\Upsilon^v(x_1)\,4\,m_1^2\,p^2\,(x_3-x_2)\Big\},\end{aligned} \tag{A10}$$

$$\begin{aligned}\mathcal{A}_N^d = {} & \frac{m_3}{N_c}\int_0^1 dx_1\int_0^1 dx_2\int_0^1 dx_3\int_0^\infty db_1\int_0^\infty b_2 db_2\int_0^\infty b_3 db_3 \\ & \phi_\Upsilon^T(x_1)\,\phi_{B_c}(x_2)\,E_n(t_d)\,\alpha_s(t_d)\,C_2(t_d)\,H_n(\alpha_e,\beta_d,b_2,b_3) \\ & \delta(b_1-b_2)\Big\{\phi_\rho^V(x_3)\,m_2\Big[2\,m_1^2\,x_1-t\,x_2-u\,x_3\Big] \\ & +2\,m_1\,m_2\,p\,\phi_\rho^A(x_3)\,(x_2-x_3)\Big\},\end{aligned} \tag{A11}$$

$$\begin{aligned}\mathcal{A}_T^d = {} & \frac{m_3}{N_c\,p}\int_0^1 dx_1\int_0^1 dx_2\int_0^1 dx_3\int_0^\infty db_1\int_0^\infty b_2 db_2\int_0^\infty b_3 db_3 \\ & \phi_\Upsilon^T(x_1)\,\phi_{B_c}(x_2)\,E_n(t_d)\,\alpha_s(t_d)\,C_2(t_d)\,H_n(\alpha_e,\beta_d,b_2,b_3) \\ & \delta(b_1-b_2)\Big\{\phi_\rho^A(x_3)\,r_2\Big[2\,m_1^2\,x_1-t\,x_2-u\,x_3\Big] \\ & +2\,m_2\,p\,\phi_\rho^V(x_3)\,(x_2-x_3)\Big\},\end{aligned} \tag{A12}$$

where $\bar{x}_i = 1 - x_i$; variable x_i and b_i are the longitudinal momentum fraction and the conjugate variable of the transverse momentum $k_{i\perp}$ of the valence quark, respectively; α_s is the QCD coupling; $a_1 = C_1 + C_2/N$; $C_{1,2}$ are the Wilson coefficients.

The function $H_{f,n}$ and Sudakov factor $E_{f,n}$ are defined as follows, where the subscripts f and n correspond to factorizable and nonfactorizable topologies, respectively.

$$H_f(\alpha_e,\beta,b_i,b_j) = K_0(\sqrt{-\alpha_e}b_i)\Big\{\theta(b_i-b_j)K_0(\sqrt{-\beta}b_i)I_0(\sqrt{-\beta}b_j)+(b_i\leftrightarrow b_j)\Big\}, \quad \text{(A13)}$$

$$\begin{aligned}H_n(\alpha_e,\beta,b_2,b_3) &= \Big\{\theta(-\beta)K_0(\sqrt{-\beta}b_3)+\frac{\pi}{2}\theta(\beta)\Big[iJ_0(\sqrt{\beta}b_3)-Y_0(\sqrt{\beta}b_3)\Big]\Big\}\\ &\times \Big\{\theta(b_2-b_3)K_0(\sqrt{-\alpha_e}b_2)I_0(\sqrt{-\alpha_e}b_3)+(b_2\leftrightarrow b_3)\Big\}, \quad \text{(A14)}\end{aligned}$$

$$E_f(w) = \exp\{-S_{B_c}(w)\}, \quad \text{(A15)}$$

$$E_n(w) = \exp\{-S_{B_c}(w)-S_\rho(w)\}, \quad \text{(A16)}$$

$$S_{B_c}(w) = s(x_2,p_2^+,1/b_2)+2\int_{1/b_2}^{w}\frac{d\mu}{\mu}\gamma_q, \quad \text{(A17)}$$

$$S_\rho(w) = s(x_3,p_3^+,1/b_3)+s(\bar{x}_3,p_3^+,1/b_3)+2\int_{1/b_3}^{w}\frac{d\mu}{\mu}\gamma_q, \quad \text{(A18)}$$

where J_0 and Y_0 (I_0 and K_0) are the (modified) Bessel function of the first and second kind, respectively; $\gamma_q=-\alpha_s/\pi$ is the quark anomalous dimension; the expression of $s(x,Q,1/b)$ can be found in the appendix of Ref.[3]; α_e is the gluon virtuality; the subscript of the quark virtuality β_i corresponds to the indices of Fig.1. The definitions of the particle virtuality and typical scale t_i are listed as follows.

$$\alpha_e = \bar{x}_1^2m_1^2+\bar{x}_2^2m_2^2-\bar{x}_1\bar{x}_2t, \quad \text{(A19)}$$

$$\beta_a = m_1^2-m_b^2+\bar{x}_2^2m_2^2-\bar{x}_2t, \quad \text{(A20)}$$

$$\beta_b = m_2^2-m_c^2+\bar{x}_1^2m_1^2-\bar{x}_1t, \quad \text{(A21)}$$

$$\begin{aligned}\beta_c &= x_1^2m_1^2+x_2^2m_2^2+\bar{x}_3^2m_3^2\\ &- x_1x_2t-x_1\bar{x}_3u+x_2\bar{x}_3s, \quad \text{(A22)}\end{aligned}$$

$$\begin{aligned}\beta_d &= x_1^2m_1^2+x_2^2m_2^2+x_3^2m_3^2\\ &- x_1x_2t-x_1x_3u+x_2x_3s, \quad \text{(A23)}\end{aligned}$$

$$t_{a(b)} = \max(\sqrt{-\alpha_e},\sqrt{-\beta_{a(b)}},1/b_1,1/b_2), \quad \text{(A24)}$$

$$t_{c(d)} = \max(\sqrt{-\alpha_e},\sqrt{|\beta_{c(d)}|},1/b_2,1/b_3). \quad \text{(A25)}$$

[1] K. Olive *et al.* (Particle Data Group), Chin. Phys. C 38, 090001 (2014).

[2] Ed. A. Bevan *et al.*, Eur. Phys. J. C 74, 3026 (2014).

[3] H. Li, Phys. Rev. D 52, 3958 (1995).

[4] C. Chang, H. Li, Phys. Rev. D 55, 5577 (1997).

[5] T. Yeh, H. Li, Phys. Rev. D 56, 1615 (1997).

[6] K. Sharma, R. Verma, Int. J. Mod. Phys. A 14, 937 (1999).

[7] R. Dhir, R. Verma, A. Sharma, Adv. in High Energy Phys. 2013, 706543 (2013).

[8] M. Beneke *et al.*, Phys. Rev. Lett. 83, 1914 (1999).

[9] M. Beneke *et al.*, Nucl. Phys. B 591, 313 (2000).

[10] M. Beneke *et al.*, Nucl. Phys. B 606, 245 (2001).

[11] C. Bauer *et al.*, Phys. Rev. D 63, 114020 (2001).

[12] C. Bauer, D. Pirjol, I. Stewart, Phys. Rev. D 65, 054022 (2002).

[13] C. Bauer *et al.*, Phys. Rev. D 66, 014017 (2002).

[14] M. Beneke *et al.*, Nucl. Phys. B 643, 431 (2002).

[15] G. Buchalla, A. Buras, M. Lautenbacher, Rev. Mod. Phys. 68, 1125, (1996).

[16] G. Lepage, S. Brodsky, Phys. Rev. D 22, 2157 (1980).

[17] T. Kurimoto, H. Li, A. Sanda, Phys. Rev. D 65, 014007 (2001).

[18] P. Ball, G. Jones, JHEP, 0703, 069, (2007).

[19] G. Lepage *et al.*, Phys. Rev. D 46, 4052 (1992).

[20] G. Bodwin, E. Braaten, G. Lepage, Phys. Rev. D 51, 1125 (1995).

[21] N. Brambilla *et al.*, Rev. Mod. Phys. 77, 1423 (2005).

[22] B. Xiao, X. Qin, B. Ma, Eur. Phys. J. A 15, 523 (2002).

[23] J. Sun *et al.*, Phys. Rev. D 92, 074028 (2015).

[24] C. Chen, Y. Keum, H. Li, Phys. Rev. D 66, 054013 (2002)

[25] T. Chiu, T. Hsieh, C. Huang, K. Ogawa, Phys. Lett. B 651, 171 (2007).

[26] R. Aaij *et al.* (LHCb Collaboration), JHEP 1407, 094 (2014).

[27] B. Abelev *et al.* (ALICE Collaboration), Phys. Lett. B 740, 105 (2015).